Temperature dependence of nonradiative recombination in low-band gap $In_xGa_{1-x}As/InAs_yP_{1-y}$ double heterostructures grown on InP substrates

T. H. Gfroerer[a] and L. P. Priestley
Department of Physics, Davidson College, Davidson, North Carolina 28035

M. F. Fairley[b]
Spelman College, Atlanta, Georgia 30314

M. W. Wanlass
National Renewable Energy Laboratory, Golden, Colorado 80401

(Received 27 March 2003; accepted 28 April 2003)

We have used photoexcitation-dependent radiative efficiency measurements to investigate the rates of defect-related, radiative, and Auger recombination in lattice-matched $In_xGa_{1-x}As/InAs_yP_{1-y}$ double heterostructures on InP substrates. Temperature dependence is used to discern the underlying mechanisms responsible for the nonradiative recombination processes. We find that defect-related recombination decreases with an increase in the temperature when the epistructure is lattice matched to the substrate ($x=0.53$). In contrast, when the epistructure is lattice mismatched to the substrate, defect-related recombination increases slowly with the temperature. The difference between the lattice-matched and mismatched cases is related to fundamental changes in the defect-related density of states function. The temperature dependence in the lattice-mismatched structures is attributed to two competing effects: wider carrier diffusion, which augments the capture rate, and thermally activated escape, which reduces the occupation of shallow traps. The band gap and temperature dependence of the Auger rate demonstrate that the conduction to heavy hole band/splitoff to heavy hole band mechanism generally dominates Auger recombination in undoped low-band gap $In_xGa_{1-x}As$. With this interpretation, our results give a spin–orbit valence split-off band effective mass of $m_{so}=(0.12\pm0.02)m_0$. © *2003 American Institute of Physics.*
[DOI: 10.1063/1.1586468]

INTRODUCTION

Low band gap $In_xGa_{1-x}As$ is important for a variety of infrared technologies. When the ternary alloy is lattice matched to InP ($x=0.53$), the band gap energy coincides with a major optical communications band where optical fiber loss and dispersion are minimal. Lattice-mismatched indium-rich $In_xGa_{1-x}As$ alloys extend the operation of InGaAs/InP-based devices deeper into the infrared, enabling new technologies like thermophotovoltaic (TPV) energy conversion. However, lattice-mismatched epistructures tend to contain a high density of defects, which often facilitate rapid nonradiative recombination. Defect-related trapping and recombination limit the performance of almost all semiconductor devices. Among other detrimental effects, trapping and nonradiative recombination at defects restrict minority carrier transport and contribute to localized heating. These problems can be alleviated somewhat by including a special step-graded region between the substrate and the device.[1] In these devices, defect states appear to be concentrated near the band edges where the traps are less effective and nonradiative recombination through the intermediate defect levels is less efficient.[2]

Changes in the nature and concentration of defects alter the rate of Shockley–Read–Hall (SRH) recombination,[3] but changes in alloy composition primarily affect Auger recombination, which depends heavily on the band structure. The likelihood of band-to-band Auger scattering increases dramatically with a decrease in band gap energy and an increase in temperature,[4] so room-temperature devices based on narrow band gap materials are often limited by rapid Auger recombination. A wide variety of Auger processes can occur in a semiconductor depending on the doping concentration and the band structure.[5] Theoretical predictions for the dominant Auger mechanism in bulk, undoped InGaAs do not agree. Dutta and Nelson suggested that the conduction to heavy hole band/conduction to conduction band (CHCC) process has the largest rate,[4] but Gel'mont *et al.*[6] and Haug[7] have disputed this result. Gel'mont *et al.* found the conduction to heavy hole band/split-off to heavy hole band (CHSH) mechanism dominant,[6] while Haug determined that phonon-assisted CHCC was most important.[7] It should be noted that these predictions depend on the alloy composition, carrier density, and temperature.

Experimental results are more consistent, and they indicate that the CHSH Auger process generally dominates in bulk $In_{0.53}Ga_{0.47}As$.[8,9] The Auger rate in undoped, lattice-matched InGaAs/InP quantum wells shows little temperature dependence, suggesting that a phonon-mediated mechanism

[a]Electronic mail: tigfroerer@davidson.edu
[b]Work done at Davidson College.

 © 2003 American Institute of Physics

Downloaded 08 Nov 2005 to 152.42.169.207. Redistribution subject to AIP license or copyright, see http://jap.aip.org/jap/copyright.jsp

TABLE I. Sample structure with nominal growth parameters. Individual samples are identified by the $In_xGa_{1-x}As$ band gap energy averaged over a range of temperatures (77–296 K).

Undoped $InAs_yP_{1-y}$, 30 nm
Undoped $In_xGa_{1-x}As$, 1.5 μm
Undoped $InAs_yP_{1-y}$ buffer, 1 μm
Undoped $InAs_yP_{1-y}$ step-grade region: 0.3 μm/step (LMM/step≈−0.2%), n steps
Undoped InP substrate

Nominal epistructure parameters

Average E_g (eV)	x	y	LMM (%)	n
0.77	0.53	0	0	0
0.71	0.60	0.14	−0.46	2
0.65	0.66	0.27	−0.87	4
0.56	0.78	0.53	−1.69	8

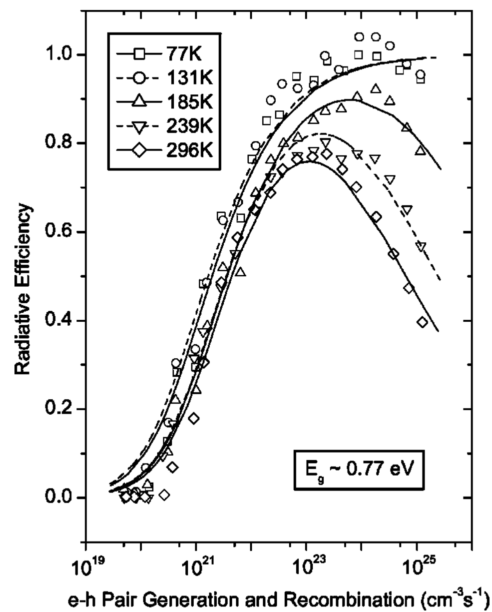

FIG. 1. Internal radiative quantum efficiency (integrated PL intensity divided by the excitation power) vs the steady-state rate of electron-hole pair generation and recombination in the nominally lattice-matched epistructure. The solid and dashed curves are theoretical fits to the data.

is most important in the quantum-confined case.[9] Recently the compositional dependence of Auger recombination was measured in low-band gap, degenerate n-type $In_xGa_{1-x}As$ and was shown to be consistent with a phonon-assisted CHCC mechanism.[10] In this article, we report a comprehensive investigation of how temperature *and* composition affect the Auger rate in bulk, undoped $In_xGa_{1-x}As$. The combination of composition and temperature dependence provides a valuable crosscheck on interpretation of our results.

EXPERIMENT

Our samples are based on the following design: a lattice-matched (LM) $InAs_yP_{1-y}/In_xGa_{1-x}As/InAs_yP_{1-y}$ double-heterostructure device (LM when $y=2.14x-1.14$)[11] is grown lattice mismatched (LMM) on an InP substrate with an intervening compositionally step-graded region of $InAs_yP_{1-y}$. The low-band gap $In_xGa_{1-x}As$ alloy serves as the light absorber/emitter and the LM $InAs_yP_{1-y}$ cladding layers passivate the interfaces and confine carriers in the $In_xGa_{1-x}As$ material. Deleterious effects of the LMM (e.g., dislocation formation and morphological defects) are alleviated by including an appropriate number of −0.2% mismatch $InAs_yP_{1-y}$ steps between the substrate and the double-heterostructure device. The lowest band gap (~0.5 eV at room temperature) $In_xGa_{1-x}As$ alloys under investigation experience severe (up to −1.7%) LMM. Our step-graded design, combined with the passivation afforded by LM $InAs_yP_{1-y}$ cladding layers, has resulted in dramatic improvements in TPV converter performance.[11] In this work, we report photoexcitation-dependent radiative efficiency measurements on several different epistructures that range from the LM condition ($x=0.53$) where no grading is employed to step-graded structures accommodating significant LMM ($x=0.60$, 0.66, and 0.78). A schematic and details of the sample structures are given in Table I.

Calibrated radiative efficiency measurements over a range of temperatures are used to study how the SRH and Auger recombination processes compete with radiative events. Previous work has shown that these structures produce strong band-to-band photoluminescence and generally have minority carrier lifetimes in excess of 1 μs at room temperature.[1] Since radiative recombination is even faster at low temperatures and SRH recombination saturates at high carrier densities, we assume that the 77 K, high-excitation measurements are close to 100% internal quantum efficiency. Auger recombination, which can be important at high-carrier density, is expected to be slow in the low temperature regime. The low-temperature, high-carrier density result provides a baseline for calibrating measurements at other temperatures and excitation intensities. We measure the relative integrated photoluminescence (PL) signal r_{PL} (corrected for detector response) as a function of the photoexcitation intensity, and plot the ratio r_{PL}/r_{gen} against the carrier generation rate $r_{gen}=I_{abs}/(E_{ex}V)$. In this latter expression, I_{abs} is the intensity of the absorbed laser light, E_{ex} is the laser energy ($\lambda=1064$ nm), and V is the photoexcited volume. The laser spot has a 0.039 cm full width at half maximum (FWHM) Gaussian profile and this width is used as an approximate measure of the diameter of V. Representative experimental data are shown in Figs. 1 and 2.

THEORY

The net rate of carrier recombination varies with carrier density n as

$$r_{rec}=A(n)+\frac{B}{N}n^2+Cn^3, \qquad (1)$$

where $A(n)$, B, and C characterize the rates of defect-related, radiative, and Auger recombination, respectively. The photon recycling factor N is the average number of radiative recombination events required for a photon to escape

Downloaded 08 Nov 2005 to 152.42.169.207. Redistribution subject to AIP license or copyright, see http://jap.aip.org/jap/copyright.jsp

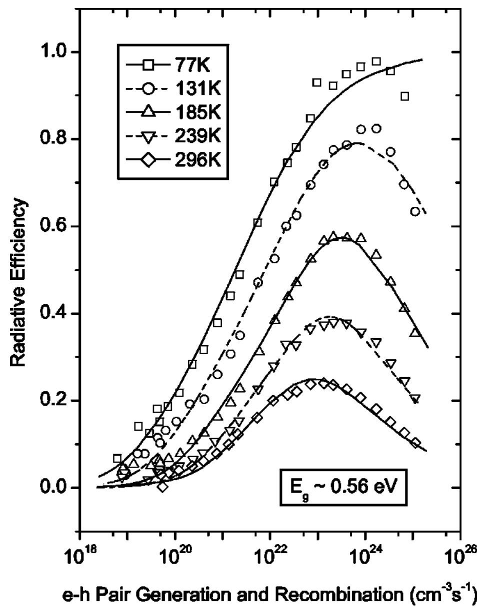

FIG. 2. Internal radiative quantum efficiency vs the steady-state rate of electron-hole pair generation and recombination in the lowest band gap lattice-mismatched epistructure. The solid and dashed curves are theoretical fits to the data.

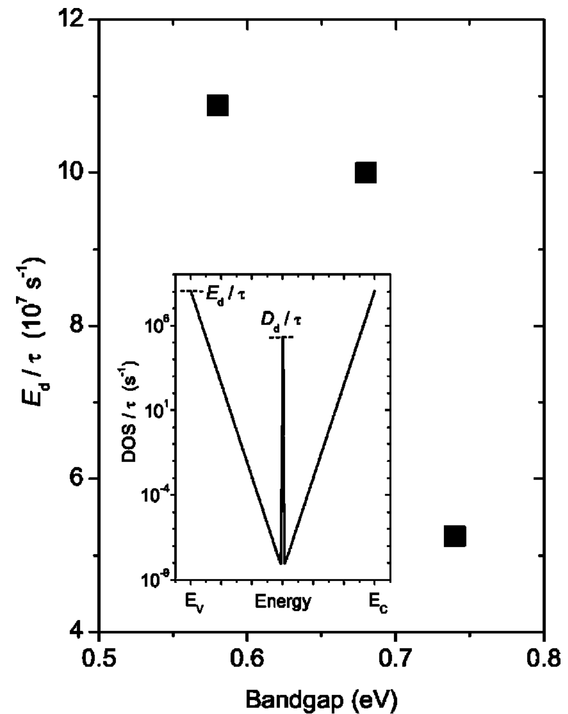

FIG. 3. Near-band edge recombination coefficient E_d/τ vs the $In_xGa_{1-x}As$ band gap energy in LMM structures. The defect-related DOS function (divided by capture time τ) that specifies the relationship between E_d and D_d is shown in the inset. The center spike in the DOS is a delta function with integral D_d/τ.

the photoexcited region. While the overlap of the PL and absorption spectra depends on the temperature, we estimate an average absorption coefficient[12] of 5×10^3 cm^{-1} for luminescence in $In_xGa_{1-x}As$ and calculate $N=4$ in our device by numerically averaging over photon trajectories. For this calculation, escaping photons include those that leave the sample and those that travel through the substrate but reflect off the lower surface, because these latter photons rarely return to the small region of original excitation where the carrier density is sufficient to provide for another radiative event. Since the three recombination mechanisms depend on different powers of n, they tend to dominate in different carrier density regimes. In addition, they each demonstrate distinct thermal behavior such that changes in the excitation-dependent efficiency curve with temperature further facilitate identification and resolution of their individual contributions. Most important, the temperature dependence of the coefficients that describe the nonradiative mechanisms provides insight into the recombination paths themselves.

If defect levels are concentrated near the center of the band gap, one can neglect the thermal population of band states when the Fermi energy coincides with the energy of the traps. In this case, SRH recombination statistics[3] simplify to linear dependence on carrier density: $A(n)=D_d n/2\tau$ where D_d is the number of midgap defect states and τ is the capture time. And, radiative efficiency measurements on our LM structure are consistent with this analysis. However, we have found that this treatment produces inadequate fits for our LMM structures.[2] In this latter case, good theoretical fits are only obtained when we include a relatively high concentration of defect levels near the band edges. Hence, we use the defect-related density of states (DOS) function shown in the inset of Fig. 3 to calculate $A(n)$ in the LMM structures. We note that the ratio D_d/τ changes little with the mismatched alloy composition (see Fig. 4) and assign the average 77 K value $(D_d/\tau)_{avg}=2.1\times10^5$ s^{-1} to the discrete midgap contribution. In this model, D_d continues to represent the number of midgap states while E_d provides a relative measure of the number of band edge states. Our experiment does not permit absolute measurement of D_d or E_d independent of τ so these quantities are presented together. While the functional form of the DOS function is somewhat arbitrary (other

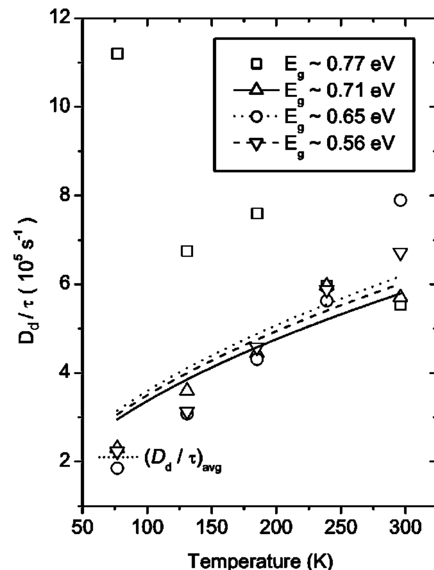

FIG. 4. Temperature dependence of D_d/τ in each of the four epistructures. Since the band gap changes with the temperature, structures are identified by an average E_g. The solid and dashed curves represent the carrier diffusion-limited model.

Downloaded 08 Nov 2005 to 152.42.169.207. Redistribution subject to AIP license or copyright, see http://jap.aip.org/jap/copyright.jsp

simple combinations of band edge and band center states also seem to work), we find that this distribution always gives good fits.

In our experiments, nonradiative recombination is measured against radiative recombination, which slows with an increase in temperature. Recombining free carriers must have equal and opposite momenta, a condition that decreases in likelihood as the average thermal energy increases. In addition, the radiative rate is proportional to the density of photon modes that can participate.[13] Quantitatively, the radiative coefficient B for free carriers should vary as[14]

$$B \propto E_g^2/(kT)^{3/2}. \tag{2}$$

This temperature dependence ($B \propto T^{-3/2}$) has been observed experimentally in lattice-matched InGaAs/InP,[12] although it should be noted that those authors did not fit their data to this form. It should also be noted that, due to the small binding energy of excitons in InGaAs ($E_{ex} \approx 2$ meV),[15] excitonic effects will not be important in the temperature range of our experiments ($77\ \mathrm{K} \leqslant T \leqslant 296\ \mathrm{K}$).

The internal radiative efficiency is defined as $Bn^2/(Nr_{rec})$. Since the radiative efficiency measurement cannot distinguish between an increase in A or C and a decrease in B, or vice versa, the theoretical behavior of B is used in the analysis. We adjust the room temperature, lattice-matched value[16] ($B = 1.5 \times 10^{-10}\ \mathrm{cm^3/s}$) within the context of Eq. (2), where PL spectra are used to estimate E_g.

Assuming a PL spectrum of functional form,

$$I_{PL}(h\nu) \propto e^{(h\nu - E_g)} \sqrt{h\nu - E_g} \tag{3}$$

yields $E_g = h\nu_{PLpeak} - kT/2$. B also depends on the effective mass of the participating electron and hole. Changes in effective mass with alloy composition are complex, especially in the valence band where strain can split the degeneracy of heavy and light holes and produce an anisotropic band structure.[17] Still, the average hole mass does not change appreciably and the effective mass of the electron is too small to make a significant contribution.[18] Hence, we neglect the variation of B with the effective mass in our analysis.

RESULTS

We start with our 77 K measurements where Auger recombination can be neglected and use a least-squares fitting procedure to obtain the best E_d/τ values for each structure. Since D_d and E_d are fixed for a given sample (the density of defect-related states does not depend on the temperature), we then fit the higher temperature data with τ and C as adjustable parameters (see Figs. 1 and 2 for representative fits). The continued success of the model over a wide range of higher temperatures provides further evidence that our modified DOS interpretation is correct. We should note that our absolute values for D_d/τ, E_d/τ, and C are subject to some uncertainty because they depend on several approximations including our estimate of the photon recycling factor N. Nevertheless, in this work we are primarily concerned with temperature and/or band gap dependent *changes* in these parameters, which should not depend on these approximations and do not depend on N.

The band gap dependence of E_d in the LMM structures is shown in Fig. 3 ($E_d \approx 0$ for the LM structure because inclusion of near-band edge states does not yield better fits). The increase in E_d with a decrease in band gap suggests that the density of near-band edge defect levels grows with an increase in lattice mismatch between the substrate and the epistructure. This phenomenon is consistent with our attribution of the new levels to structural changes that accompany lattice mismatch. The temperature dependence of D_d/τ for each of the structures under investigation is shown in Fig. 4. The quantitative agreement among the LMM structures demonstrates a surprising feature of this system: the number of midgap defect states does not depend on the degree of lattice mismatch.

Defect-related recombination varies with the temperature primarily through changes in the range of diffusion of carriers and thermally activated trapping and escape processes. At higher lattice temperatures T, carriers have more kinetic energy and tend to diffuse farther before recombining. Depending on the distribution of defects, this feature may increase the probability per unit time τ^{-1} that a carrier will encounter a defect site. For example, short- and medium-range spatial fluctuations in PL intensity have been found to correlate differently with dark current in lattice-mismatched InGaAs photodiodes.[19] This phenomenon may be due to motion of carriers in the material and the relative proximity of traps. Thermally activated escape should be unimportant in the LM structure because defect levels are very deep relative to kT. However, the LMM structures have a high concentration of shallow traps. SRH recombination statistics on the defect-related DOS functions shown in Fig. 3 indicate that as T increases from 77 to 296 K, thermally activated escape reduces the defect-related recombination rate by approximately a factor of 2. This phenomenon is offset by the decrease in τ with temperature shown in Fig. 4, so that the overall rate increases slowly between 77 and 296 K.

The carrier capture rate is given by $c = \sigma \bar{v} n_T$, where σ is the capture cross section, n_T is the trap density, and $\bar{v}$ is the mean thermal velocity of the participating carriers: $\bar{v} = \sqrt{3kT/m^*}$. The solid, dotted, and dashed curves in Fig. 4 are fits to the lattice-mismatched results ($E_g \sim 0.71$, 0.65, and 0.56 eV) based on this model. If trapping is limited by electron diffusion ($m^* = 0.04 m_0$),[18] the fitting parameters give $\sigma n_T \approx 0.01\ \mathrm{cm^{-1}}$ while heavy hole[18] ($m^* = 0.46 m_0$) limited diffusion yields $\sigma n_T \approx 0.03\ \mathrm{cm^{-1}}$. If the defect centers have cross sections comparable to the dimensions of lattice sites $\sigma \approx (0.3\ \mathrm{nm})^2$, the trap concentration n_T is approximately $2 \times 10^{13}\ \mathrm{cm^{-3}}$.

The temperature dependence of D_d/τ in the LM structure ($E_g \sim 0.77$ eV) deviates considerably from that of the mismatched alloys. D_d/τ appears to decrease with the temperature in this case. Clearly, SRH recombination is not diffusion limited in the LM sample and the temperature dependence is too weak to be consistent with thermally activated capture/escape mechanisms. Hence, the apparent quenching of defect-related recombination with the temperature is difficult to explain. Nevertheless, the general results for $A(T)$ in

Downloaded 08 Nov 2005 to 152.42.169.207. Redistribution subject to AIP license or copyright, see http://jap.aip.org/jap/copyright.jsp

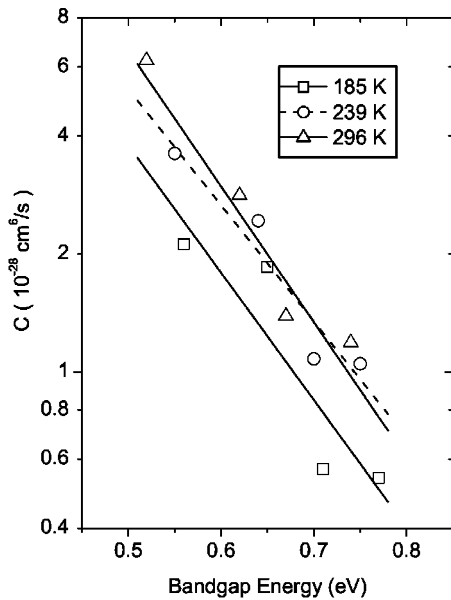

FIG. 5. Auger recombination coefficient C vs the band gap energy in $In_xGa_{1-x}As$ at several temperatures. The results clearly show the exponential dependence of C on E_g.

these structures are consistent with our previous discovery that the defect-related DOS in the LM structure is fundamentally different from that in the LMM case.[2]

The band gap and temperature dependence of the Auger coefficient C are shown in Figs. 5 and 6. The solid and dashed lines are theoretical fits to the high-temperature data. Our analysis is based on the simplest case of nondegenerate statistics and parabolic energy bands. In this case, the band-to-band Auger coefficient is expected[20] to vary as $C \propto \exp(-E_a/kT)$ where E_a is an activation energy dictated by conservation of energy and momentum. When the background density of carriers is important, the dependence of C on E_a and the temperature is more complicated.[21] However, since we are optically exciting far more carriers than the number generated thermally, exponential behavior is expected to dominate. Even though the nondegenerate assumption is suspect at the highest carrier densities and parabolic valence bands are a somewhat crude approximation in narrow-gap semiconductors, the theory fits surprisingly well. The linear fits in Fig. 6 yield an average thermal activation energy of 34±4 meV for the Auger process. While not shown in Fig. 6, we note that thermal activation of the Auger rate appears to level off at the lowest temperatures, suggesting that a phonon-mediated process becomes important for small T. This observation is consistent with the findings of Hausser *et al.*[9]

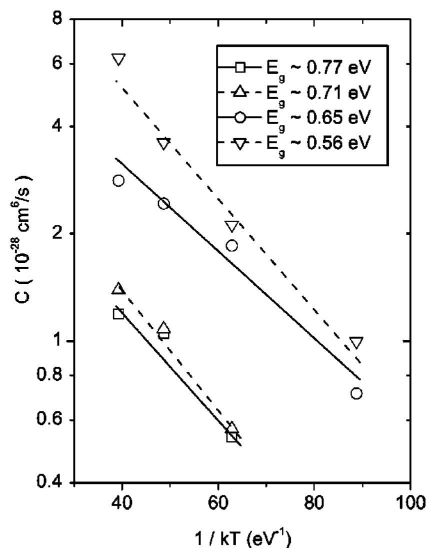

FIG. 6. Arrhenius plot of Auger recombination coefficient C in each of the four epistructures. The average thermal activation energy is 34±4 meV.

Since E_a depends on the energy separation and curvature of the participating bands, it can be used to identify which Auger mechanisms are most important. If one of the transitions involves the spin–orbit split-off band, then $E_a = \mu(E_g - \Delta)$ where μ depends on the effective mass of the participating carriers and Δ is the spin–orbit offset; otherwise, E_a is simply equal to μE_g. The average band gap dependence of C according to Fig. 5 yields $\mu = 0.15 \pm 0.04$ regardless of the underlying mechanism (the slope is independent of Δ). However, determination of μ from Fig. 6 depends on whether carriers in the split-off band participate. Since $\Delta \approx 0.34$ eV in GaAs and $\Delta \approx 0.39$ eV in InAs,[22] Δ does not vary significantly with the InGaAs composition. Using $\Delta = 0.35$ eV,[23] Auger transitions that involve excitation of holes to the split-off band give $\mu = 0.12 \pm 0.04$. If the split-off band is not involved, the temperature dependence of C yields $\mu = 0.05 \pm 0.01$.

The two determinations of μ (via dependence on the band gap and temperature) are expected to agree, indicating that only Auger mechanisms that include the spin–orbit split-off band are consistent with our experimental results. When a transition to the split-off band is included, the band gap and temperature dependent evaluations of μ statistically agree. The small discrepancy between the mean values may be attributed to changes in effective mass and Δ with the alloy composition. We conclude that the dominant band-to-band Auger recombination path involves excitation of heavy holes to the split-off band in accordance with previous experimental work on lattice-matched InGaAs/InP.[8,9] In this case[4]

$$\mu = \frac{m_{so}}{2m_v + m_c - m_{so}}, \tag{4}$$

where m_v and m_c are the heavy hole and electron effective masses, respectively. Using the average value $\mu = 0.14 \pm 0.03$, we obtain $m_{so} = (0.12 \pm 0.02)m_0$ for the effective mass of split-off holes. While the final Auger state lies well above the split-off valence band edge, the shape of this band is not expected to deviate significantly from parabolic.[7] We know of no other reported measurement of m_{so} in bulk $In_xGa_{1-x}As$. But in the absence of strain, m_{so} is not expected to vary significantly with the alloy composition[17] and our value can be compared with findings in InAs and GaAs. Our measurement falls between two experimental determinations and a theoretical prediction. Experimental work has found $m_{so} = (0.14 \pm 0.01)m_0$ in InAs[24] and $m_{so} = (0.15 \pm 0.01)m_0$ in GaAs[25] while theoretical treatment gives $m_{so} \approx 0.11 m_0$ in GaAs.[17]

Downloaded 08 Nov 2005 to 152.42.169.207. Redistribution subject to AIP license or copyright, see http://jap.aip.org/jap/copyright.jsp

CONCLUSION

We have measured temperature dependent changes in SRH and Auger recombination in lattice-matched $In_xGa_{1-x}As/InAs_yP_{1-y}$ double heterostructures grown on InP substrates. The temperature dependence of SRH recombination changed dramatically between the LM and LMM cases. When the epistructure is LMM relative to the substrate, the variation of SRH recombination with the temperature can be attributed to a combination of thermal diffusion and thermal activation out of shallow traps. The results provide additional evidence for a previous report, which uncovered a high concentration of defect levels near the band edges in these structures.[2] While the temperature dependence in the LM structure is difficult to interpret, the deviation from LMM behavior is consistent with the disparity in the underlying defect-related DOS functions.

The Auger mechanism in all of the low-band gap $In_xGa_{1-x}As$ alloys depends strongly on the temperature, with average thermal activation energy of 34 ± 4 meV. While this feature generally points to band-to-band processes, we cannot rule out the possibility that a weak phonon-mediated mechanism is also present. Our results agree with the work of Rees *et al.* who found $E_a=39\pm5$ meV in undoped InGaAs lattice matched to InP.[8] By extending the investigation to lattice-mismatched, indium-rich alloys, we confirmed that a similar band-to-band Auger mechanism continues to operate over the composition range $0.53\leqslant x\leqslant0.78$. The extension also enabled us to study the band gap dependence of the Auger rate. By comparing the temperature and the band gap dependent results, we were able to rule out band-to-band Auger mechanisms that do not include the spin–orbit split-off band, demonstrating that the CHSH path dominates in this material.

ACKNOWLEDGMENTS

The authors would like to thank J. J. Carapella for performing MOVPE growth and Dr. Wyatt Metzger for helpful discussions. This research was supported by Research Corporation. Acknowledgement is also made to the donors of The Petroleum Research Fund, administered by the American Chemical Society, for partial support of this work.

[1] R. K. Ahrenkiel, S. W. Johnston, J. D. Webb, L. M. Gedvilas, J. J. Carapella, and M. W. Wanlass, Appl. Phys. Lett. **78**, 1092 (2001).
[2] T. H. Gfroerer, L. P. Priestley, F. E. Weindruch, and M. W. Wanlass, Appl. Phys. Lett. **80**, 4570 (2002).
[3] W. Shockley and W. T. Read, Jr., Phys. Rev. **87**, 835 (1952); R. N. Hall, *ibid.* **87**, 387 (1952).
[4] N. K. Dutta and R. J. Nelson, J. Appl. Phys. **53**, 74 (1982).
[5] P. T. Landsberg, *Recombination in Semiconductors* (Cambridge University Press, Cambridge, UK, 1991), p. 250.
[6] B. L. Gel'mont, Z. N. Sokolova, and V. B. Khalfin, Sov. Phys. Semicond. **17**, 280 (1983); B. L. Gel'mont, Z. N. Sokolova, and I. N. Yassievich, *ibid.* **16**, 382 (1982).
[7] A. Haug, Appl. Phys. Lett. **42**, 512 (1983).
[8] P. Rees, P. Blood, M. J. H. Vanhommerig, G. J. Davies, and P. J. Skevington, J. Appl. Phys. **78**, 1804 (1995).
[9] S. Hausser, G. Fuchs, A. Hangleiter, and K. Streubel, Appl. Phys. Lett. **56**, 913 (1990).
[10] W. K. Metzger, M. W. Wanlass, R. J. Ellington, R. K. Ahrenkiel, and J. J. Carapella, Appl. Phys. Lett. **79**, 3272 (2001).
[11] M. W. Wanlass, J. J. Carapella, A. Duda, K. Emery, L. Gedvilas, T. Moriarty, S. Ward, J. D. Webb, X. Wu, and C. S. Murray, AIP Conf. Proc. **460**, 132 (1999).
[12] E. Zielinski, H. Schweizer, K. Streubel, H. Eisele, and G. Weimann, J. Appl. Phys. **59**, 2196 (1986).
[13] P. T. Landsberg, in Ref. 5, p. 333.
[14] R. N. Hall, Proc. Inst. Electr. Eng. **B106** (Suppl. 17), 923 (1959).
[15] S. Adachi, *Physical Properties of III–V Semiconductor Compounds* (Wiley, New York, 1992), p. 157.
[16] T. H. Gfroerer, E. A. Cornell, and M. W. Wanlass, J. Appl. Phys. **84**, 5360 (1998).
[17] J. Singh, in *Properties of Lattice-Matched and Strained Indium Gallium Arsenide*, edited by P. Bhattacharya (INSPEC, London, 1993), p. 97.
[18] S. Adachi, in Ref. 15, pp. 86–96.
[19] S. K. Krawczyk, K. Schohe, C. Klingelhofer, B. Vilotitch, C. Lenoble, M. Villard, X. Hugon, D. Regaud, and F. Ducroquet, *Indium Phosphide and Related Materials* (IEEE, New York, 1990), p. 265.
[20] P. T. Landsberg, in Ref. 13, p. 253.
[21] P. T. Landsberg, in Ref. 13, p. 300.
[22] Landolt–Bornstein, *Numerical Data and Functional Relationships in Science and Technology* (Springer, New York, 1982), Vol. 17, Subvol. a, pp. 220 and 298.
[23] S. Adachi, in Ref. 15, p. 81.
[24] C. R. Pidgeon, S. H. Groves, and J. Feinleib, Solid State Commun. **5**, 677 (1967).
[25] M. Reine, R. L. Aggarwal, B. Lax, and C. M. Wolfe, Phys. Rev. B **2**, 458 (1970).

Downloaded 08 Nov 2005 to 152.42.169.207. Redistribution subject to AIP license or copyright, see http://jap.aip.org/jap/copyright.jsp